

# A Novel Glycolipid and Phospholipid in the Purple Membrane<sup>†</sup>

Angela Corcelli,\*<sup>‡</sup> Matilde Colella,<sup>‡</sup> Giuseppe Mascolo,<sup>§</sup> Francesco Paolo Fanizzi,<sup>||</sup> and Morris Kates<sup>⊥</sup>

Dipartimento di Fisiologia Generale ed Ambientale, Università di Bari, Bari, Italy, Dipartimento Farmaco-Chimico, Università di Bari, Bari, and Consortium CARSO, Cancer Research Center, Valenzano-Bari, Italy, IRSA-CNR, Bari, Italy, and Department of Biochemistry, Microbiology and Immunology, University of Ottawa, Ottawa, Canada

Received October 22, 1999; Revised Manuscript Received December 23, 1999

**ABSTRACT:** A novel glycolipid of mass 1935 and a phospholipid of mass 1522 are the main residual lipids (along with traces of PGP-Me, S-TGD-1, and PG) specifically associated with “delipidated” bacteriorhodopsin fractions BR I and BR II, prepared by Triton X-100 treatment of purple membrane (PM), from a genetically engineered strain (L33) of *Halobacterium salinarum*, and chromatography on phenyl-Sepharose CL-4B. The novel glycolipid and phospholipid are components of the PM matrix not previously described. The TLC isolated and purified novel glycolipid and phospholipid were shown, by chemical degradation, mass spectrometry, and NMR analyses, to have the structure, respectively, of a phosphosulfoglycolipid, 3-HSO<sub>3</sub>-Galp-β1,6Manp-α1,2Glc-α1,1-[sn-2,3-di-*O*-phytanylglycerol]-6-[phospho-sn-2,3-di-*O*-phytanylglycerol], and of a glycerol diether analogue of bisphosphatidylglycerol (cardiolipin), sn-2,3-di-*O*-phytanyl-1-phosphoglycerol-3-phospho-sn-2,3-di-*O*-phytanylglycerol.

Using the purple membrane from a genetically engineered strain (L33) of *Halobacterium salinarum* (1), we have recently reported the isolation of “delipidated” bacteriorhodopsin fractions BR I<sup>1</sup> and BR II by treatment of PM with Triton X-100 and chromatography on phenyl-Sepharose CL-4B, and have described some of their functional characteristics (2). Although 90% of the phospholipids were removed by this procedure, BR I and BR II fractions showed functionally different properties attributable to their different residual phospholipid:protein molar ratios. Light adaptation studies and circular dichroism measurements indicated that BR I consists of bacteriorhodopsin trimers, while BR II contains mainly monomers (2). Formation of these two species of BR probably arose from the fact that the delipidation process is not capable of removing all of the

phospholipids that maintain the trimer structure of PM, so that the conversion of trimers (BR I) to monomers (BR II) is incomplete. It was therefore of interest to identify the phospholipid and glycolipid components of the residual lipids that are resistant to the delipidation procedure used here and might have a role in stabilizing the trimer structure.

TLC analysis of the residual lipids associated with delipidated bacteriorhodopsin revealed the presence of a new glycolipid and a new phospholipid in the purple membrane, in addition to the phospholipids (PG, PGS, and PGP-Me) and glycolipids (S-TGD-1) previously reported for PM (3–5). The new glycolipid and phospholipid have not previously been reported as lipid components of the PM prepared from *Halobacterium cutirubrum* (type strain NRC 34001) (3) or *Halobacterium halobium* (strain R1) (4), but appear to be the main lipids associated with delipidated bacteriorhodopsin prepared from the genetically engineered strain (L33) of *Hb. salinarum* (1) used here.

In the present paper we describe the identification of the lipids associated with BR I and BR II and also the detailed structure determination of the two new lipids by conventional analytical and spectroscopic methods and by identification of their acid degradation products. The glycolipid was shown to be a diphytanylglycerol ether analogue of a phosphosulfoglycolipid, and the phospholipid is a diphytanylglycerol ether analogue of cardiolipin.

## EXPERIMENTAL PROCEDURES

**Materials.** DNase and *n*-octyl-β-glucopyranoside (octyl glucoside, OG) were from Sigma, sodium cholate was from Serva, and phenyl-Sepharose CL-4B was from Pharmacia. All organic solvents used were commercially distilled and of the highest available purity (Sigma-Aldrich). TLC plates (60A) and HPTLC (60A) plates, obtained from Merck, were washed twice with chloroform/methanol (1:1, v/v) and

<sup>†</sup> Supported by the Ministero Italiano dell'Università e della Ricerca Scientifica (MURST) and Centro Studi Chimico Fisici sull'Interazione Luce-Materia (CNR), 70126 Bari, Italy.

\* To whom correspondence should be addressed. Phone: 39 80 544 3335. Fax: 39 80 544 3388. E-mail: a.corcelli@biologia.uniba.it.

<sup>‡</sup> Dipartimento di Fisiologia Generale ed Ambientale, Università di Bari.

<sup>§</sup> IRSA, CNR.

<sup>||</sup> Dipartimento Farmaco-Chimico, Università di Bari, and Cancer Research Center.

<sup>⊥</sup> University of Ottawa.

<sup>1</sup> Abbreviations: BPG, bisphosphatidylglycerol (cardiolipin) (diphytanylglycerol analog); BR, bacteriorhodopsin; CID-MS, chemical ionization mass spectrometry; COSYDFT, double-quantum-filtered-phase-sensitive correlation spectroscopy; COSYGS, gradient accelerated COSY; DEPT, distortionless enhancement by polarization transfer; DPG, sn-2,3-di-*O*-phytanylglycerol; ESI-MS, electrospray ionization mass spectrometry; HPLC, high-performance liquid chromatography; HPTLC, high-performance thin-layer chromatography; NMR, nuclear magnetic resonance spectroscopy; OG, octyl glucoside; PA, phosphatidic acid (diphytanylglycerol ether analog); PG, phosphatidylglycerol (diphytanylglycerol ether analog); PGP-Me, phosphatidylglycerophosphate methyl ester (diphytanylglycerol ether analog); PM, purple membrane; PGS, phosphatidylglycerosulfate (diphytanylglycerol ether analog); S-TGD-1, 3-HSO<sub>3</sub>-Galp-β1,6-Manp-α1,2-Glc-α1,1-sn-2,3-diphytanylglycerol; TLC, thin-layer chromatography.

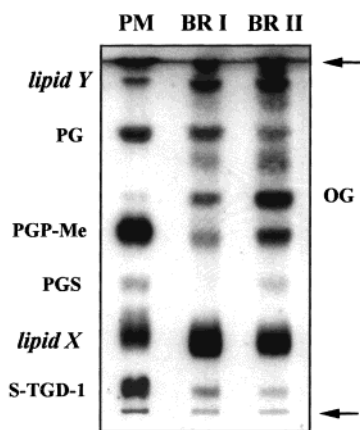


FIGURE 1: TLC plate of lipid extracts of purple membrane (PM) and of bacteriorhodopsin fractions isolated on phenyl-Sepharose CL-4B (BR I and BR II). The plate was developed with solvent A (chloroform/methanol/90% acetic acid, 65:4:35, v/v). The chromatogram was charred with 0.5% sulfuric acid/ETOH. OG = octylglucoside. The spot between OG and PG and the other at the front present in BR I and II, but not in PM, are not identified lipid degradation products. Lipid X and lipid Y are unidentified lipids enriched in delipidated BR fractions.

activated at 120 °C before use. Lipid standards of diphytanylglycerol ether ( $C_{20}$ – $C_{20}$ ) (DPG) and diphytanylglycerol ether analogues of phosphatidic acid (PA), phosphatidylglycerophosphate methyl ester (PGP-Me), and sulfoglycolipid (S-TGD-1) were prepared as described elsewhere (6).

**Culture of Microorganism.** A genetically engineered high-BR-producing strain (L33) of *Hb. salinarum*, a gift from Richard Needleman (1), was grown in light at 37 °C in a liquid growth medium, containing neutralized peptone (L34, Oxoid), prepared as previously described (7).

**Bacteriorhodopsin Isolation.** Purple membrane (PM), isolated as described previously (7), was treated with Triton X-100, and the delipidated bacteriorhodopsin fractions (BR I and BR II) were isolated by chromatography on phenyl-Sepharose CL-4B eluted with octyl glucoside, as described elsewhere (2). Detergent associated with delipidated BR fractions was removed by dialysis against distilled water, before lipid extraction, but some octyl glucoside still remained in the preparations (see Figure 1).

**Lipid Extraction.** Total PM lipids and residual lipids associated with the delipidated bacteriorhodopsin BR I and BR II were extracted by the method of Bligh and Dyer (8), as modified for extreme halophiles (6,9).

**Thin-Layer Chromatography.** Preparative TLC of total lipid extracts was carried out on silica gel 60A plates (Merck, 20 × 20 cm × 0.5 mm thick layer) in solvent A (chloroform/methanol/90% acetic acid, 65:4:35, v/v). Rechromatography of individual lipids was carried out on silica gel 60A plates (10 × 20 cm × 0.25 mm) in neutral solvent B (chloroform/methanol/water, 65:25:4, v/v). Lipids were detected with the following spray reagents (9): (a) molybdenum blue Sigma spray reagent for phospholipids; (b) 0.5% orcinol/sulfuric acid for glycolipids; (c) azure A/sulfuric acid for sulfatides and sulfoglycolipids (10); (d) ninhydrin in acetone/lutidine (9:1) for free amino groups; (e) hydroxylamine–FeCl<sub>3</sub> reagent for amides; (f) 0.5% sulfuric acid in ethanol, followed by charring at 120 °C, for all lipids. Lipids on preparative TLC plates were visualized by staining with iodine vapor.

**Isolation and Purification of the Unknown Glycolipid and Phospholipid.** The lipid components of PM and delipidated BR fractions were separated by preparative TLC in solvent A and were eluted and recovered from the silica as described elsewhere (9). Each component was finally purified by TLC in neutral solvent B and recovered from the silica as just described. The purity of the final material was checked by means of silica gel 60A HPTLC in solvent A.

**Analysis of Hydrolysis Products.** (1) *Strong Acid Methanolysis.* Purified lipids were subjected to acid methanolysis in methanolic 2 N HCl under reflux at 90 °C for 5 h in a screw cap Teflon-lined tube (9). After addition of 10% water, the mixture was extracted with hexane, and the hexane-soluble lipids were analyzed on TLC in solvent C (hexane/ethyl ether/glacial acetic acid, 70:30:1, v/v) for neutral lipids and in solvent A for polar lipids. The lipid hydrolysis products were also subjected to ESI-MS analysis. The methanol/water phase of each hydrolyzate was taken to dryness under nitrogen, and the residue was heated in 1 N aqueous HCl at 100 °C for 2 h to hydrolyze sugar methylglucosides. After complete removal of HCl the dry residue was analyzed by HPLC (Dionex system) on Carbo-Pack MA-1 and Carbo-Pack PA-1 (Dionex Corp.) columns to detect monosaccharides and phosphorylated sugar derivatives, respectively.

(2) *Mild Acid Hydrolysis.* Time course studies of partial methanolysis of the unknown glycolipid were done in 0.1 N methanolic HCl at 25 °C. Samples were taken at 1, 5, and 20 h and checked by both TLC in solvent A and ESI-MS for partial lipid hydrolysis products. Individual lipid hydrolysis products obtained after 20 h were isolated by preparative TLC and subjected to ESI-MS analysis.

**Phosphorus Quantitation.** Organically bound phosphorus was analyzed by the method of Bartlett (11).

**Retinal Quantitation.** Retinal content in the lipid extract of purple membrane, BR I, and BR II was determined spectrophotometrically (12).

**Mass Spectrometry.** Dried samples of total PM lipids, residual lipids of BR I and BR II, purified individual lipids, and lipid hydrolysis products were dissolved in chloroform/methanol (1:1) for ESI-mass spectrometry analyses. Electrospray mass spectra (ES-MS) were obtained with an API 165 mass spectrometer (Perkin-Elmer Sciex, Concord, Ontario, Canada) equipped with an ion-spray interface. The samples were continuously introduced into the mass spectrometer at a flow rate of 10  $\mu$ L/min by a Harvard model 11 syringe pump (South Natick, MA). The instrumental conditions were as follows: nebulizer gas flow (air), 1.2 L/min; curtain gas flow (nitrogen), 1.2 L/min; needle voltage, 5600 V; orifice voltage, –150 V; ring voltage, –200 V; mass range, 50–2000 amu in steps, 0.1 amu; dwell time, 0.2 ms. With the orifice voltage used, CID-MS spectra were obtained showing  $[M - H]^-$  and  $[M - 2H]^{2-}$  parent ions as well as some fragmentation ions.

**NMR Spectroscopy.** NMR spectra of isolated PM lipids were taken in CDCl<sub>3</sub>/CD<sub>3</sub>OD (4:3, v/v; final lipid concentration about 3 mM). All NMR analyses were performed on a DRX500 Avance Bruker instrument equipped with inverse probes for inverse detection and with a  $z$  gradient for gradient-accelerated spectroscopy. <sup>1</sup>H and <sup>1</sup>H-decoupled <sup>13</sup>C chemical shifts are given relative to TMS as internal standard; <sup>1</sup>H-decoupled <sup>13</sup>P chemical shifts are relative to 85% H<sub>3</sub>PO<sub>4</sub>.

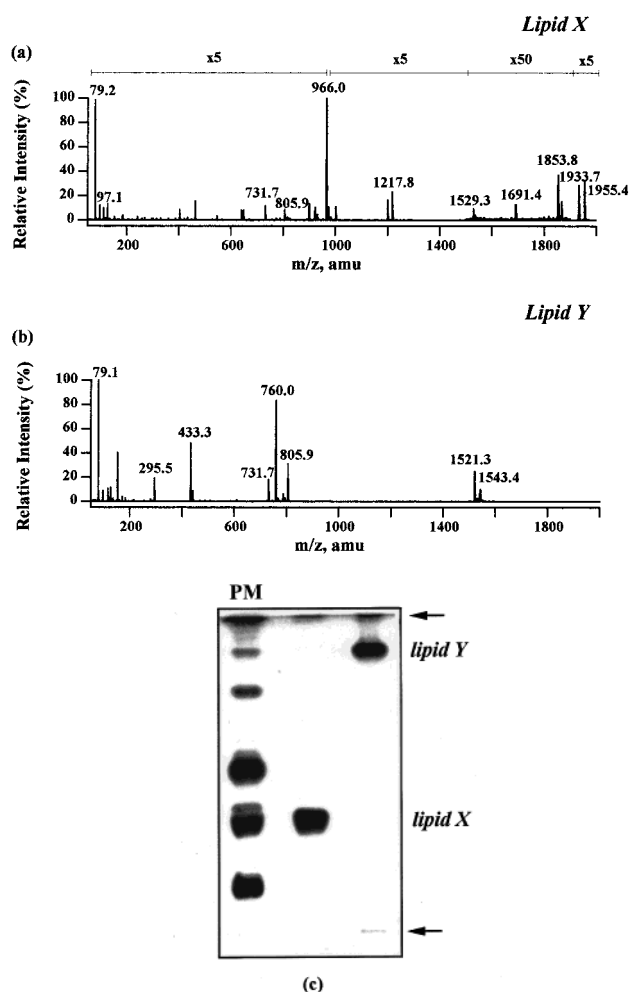


FIGURE 2: Negative-ion ESI-MS mass spectra (a, b) and TLC in solvent A (c) of purified lipid X and purified lipid Y. Staining as in Figure 1.

as external standard. Standard Bruker automation programs were used for  $^{13}\text{C}$  DEPT-135 and 2D NMR experiments. 2D COSY experiments were performed by using COSYD-FTP (double-quantum-filtered phase-sensitive COSY) and COSYGS (gradient-accelerated COSY) sequences. Inverse detected  $^1\text{H}$ – $^{13}\text{C}$  heterocorrelated 2D NMR spectra were obtained by using the gradient-sensitivity-enhanced pulse sequence INVIEAGASSI.

## RESULTS

(a) *Analysis of Residual Lipids Associated with Isolated Bacteriorhodopsin.* The lipid composition of the purple membrane and of the residual lipids in the isolated bacteriorhodopsin fractions BR I and BR II was examined by thin-layer chromatography (TLC) (Figure 1) and by electrospray mass spectrometry (ESI-MS) (Figure 3). The individual components isolated from the TLC plate (Figure 1) were identified by their  $R_f$  values relative to those of authentic standard markers, by their staining behavior with specific reagents, by their P:lipid and sugar:lipid molar ratios, and by their mass spectra. All of the components, except two, were identified as PGP-Me, PG, PGS, and S-TGD-1 (Figure 1, Table 1), which have previously been reported for purple membrane lipids of *Hb. cutirubrum* and *Hb. halobium* (3,4). The unidentified lipids, labeled “lipid X” and “lipid Y” were the major components among the residual lipids associated

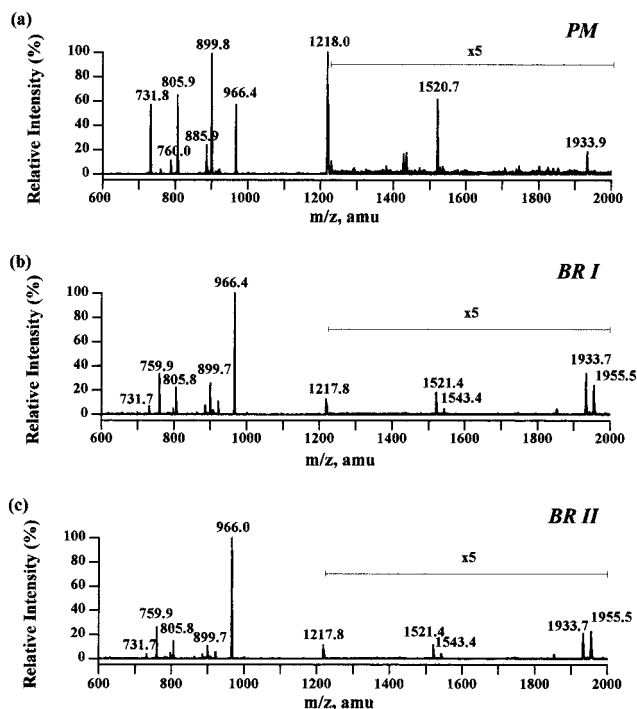


FIGURE 3: Negative-ion ESI mass spectra of total lipids of (a) PM, (b) BR I, and (c) BR II. The samples analyzed were the same as those used for TLC (Figure 1).

with BR I and BR II, but were present in relatively lower amounts in PM (Figure 1). The ESI mass spectrum of lipid X (Figure 2a) showed a strong parent molecular ion peak at  $m/z$  966.0 (doubly charged) plus a corresponding smaller one at  $m/z$  1933.7 (singly charged), and that of lipid Y showed a parent ion at  $m/z$  760.0 (doubly charged) and at 1521.3 (singly charged) (Figure 2b). The two bischarged ion peaks at  $m/z$  966 and 760 were also present in the ESI mass spectrum of the total lipid extract of PM (Figure 3a) as well as in the spectra of the lipids of BR I and BR II (Figure 3b,c). They are the main peaks in the spectra of the delipidated BR residual lipids, but are less intense in those of the PM lipids. These two bischarged peaks were not detected in earlier FAB-MS studies of PM lipids (13), but the 966 peak does appear on recent ESI mass spectra of PM from the BR-overproducing strain *Hb. salinarum* S9 (Weik et al., 1998, Figure 2 (14); Essen L. O. et al., 1998, Figure 1 (15)).

The data in Figures 1 and 3 also show that the composition of residual lipids in BR I and BR II is quantitatively different from that of the purple membrane in that the former have much higher proportions of lipid X and lipid Y. This suggests that these lipids may be more resistant to solubilization by the Triton X-100 treatment and phenyl-Sepharose chromatography than the other lipid components of PM, or alternatively, that the novel lipids are more strongly bound to bacteriorhodopsin and may be involved in stabilizing the BR trimer structure. The novel lipids appear to be specific to PM, since TLC analysis of lipid extract from membrane fractions other than PM did not show the presence of these novel lipids (data not shown).

(b) *Chemical Structure Determination of the Unidentified PM Lipids.* (i) *Lipid X.* Lipid X gave a positive test on TLC plates for sugar, sulfate, and phosphate but not for amide or amino groups (Figure 1, Table 1), indicating that it is a



Table 1: ESI-MS (Negative Mode) Ion Peaks, TLC  $R_f$  in Solvent System A, and Staining Behavior of Various PM Lipid Components

lipid	obsd signals ( $m/z$ )		calcd mass	TLC $R_f$	staining <sup>a</sup>		
	$[M - H]^-$	$[M - H]^{2-}$			sugar	phosphate	sulfate
S-TGD-1	1217.8		1218.8	0.07	+	—	+
lipid X	1933.7	966.4	1933.4	0.21	+	+	+
PGS	885.9		886.6	0.36	—	+	+
PGP-Me	899.7		900.7	0.51	—	+	—
PG	805.9		806.7	0.79	—	+	—
lipid Y	1521.3	760.0	1521.3	0.94	—	+	—
neutral lipids + pigments				0.99–1			

<sup>a</sup> None of the components gave a positive reaction with the ninhydrin stain for free amino groups, or with the hydroxylamine–FeCl<sub>3</sub> stain for amide groups.

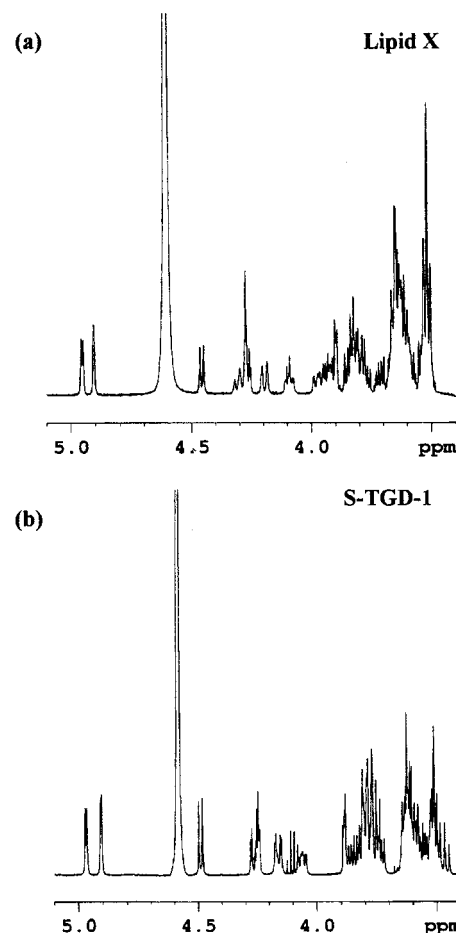
sulfoglycophospholipid. Its mobility on TLC in solvent A ( $R_f$  0.21) was higher than that of the well-known sulfotriglycosyldiphtanyl glycerol, S-TGD-1 ( $R_f$  0.07), suggesting the presence in lipid X of more hydrophobic groups or of fewer sugar groups than in S-TGD-1. Lipid X actually has a sugar:lipid molar ratio of 3:1, identical to that for S-TGD-1, and a P:lipid molar ratio of 1:1 (see the following NMR data). This indicates that lipid X has the same number of sugar groups but more hydrophobic groups than S-TGD-1 (see below).

TLC in solvent A of purified lipid X showed a single lipid component that stained positively for phosphate, sulfate, and sugar (Figure 2c).

By preparative TLC we obtained 6  $\mu$ mol of lipid X together with 6  $\mu$ mol of retinal; therefore, the molar ratio lipid X:retinal in the PM lipid extract is 1.0.

ESI (negative mode) mass spectra of the purified glycolipid (Figure 2a) showed  $[M - H]^-$  and  $[M - 2H]^{2-}$  parent ions as well as some fragmentation ions. The main ion peak is that of the bischarged molecular ion  $[M - 2H]^{2-}$  at  $m/z$  966.0, and the monocharged molecular ion ( $[M - H]^-$ ) is present at  $m/z$  1933.7 along with  $[M - 2H + Na]^-$  at  $m/z$  1955.4 as a minor peak. Fragmentation ions present at  $m/z$  79.2/97.1 are diagnostic of a phosphate group ( $[PO_3]^-/[H_2PO_4]^-$  ion pair); the less intense ion peak at  $m/z$  1853.8 is diagnostic of the loss of a labile sulfate group ( $[M - SO_3]^- = 1934 - 80 = 1854$ ). Also, four fragmentation ions present at  $m/z$  731.7, 1217.8, 1529.3, and 1691.4 correspond, respectively, to *sn*-1-phospho-2,3-di-*O*-phytanylglycerol (the analogue of phosphatidic acid, PA; MW 733), S-TGD-1 (MW 1219), the parent ion minus a sulfodiglycosyl residue ( $[M - HSO_3 - diglycosyl]^- = 1934 - 80 - 324 = 1530$ ), and the parent ion minus a sulfoglycosyl group ( $[M - HSO_3 - glycosyl]^- = 1934 - 80 - 163 = 1691$ ). The ESI-MS data thus suggest that lipid X consists of a sulfotriglycosyldiphtanylglycerol esterified to the phosphate group of PA.

Proton NMR spectra of the novel lipid X and S-TGD-1 (Figure 4) provided further evidence in support of a S-TGD/PA-linked structure. Integration of the methyl proton signals (ca. 0.8 ppm) gave 60 methyl protons for lipid X, as compared to 30 in S-TGD-1, indicating the presence in lipid X of 4 phytanyl groups (each with 5 methyl groups per chain), equivalent to 2 molecules of diphtanylglycerol. Furthermore, the spectrum of lipid X in the region characteristic of glycosyl protons (3.4–5.1 ppm) (Figure 4a) was quite similar to that of S-TGD-1 (Figure 4b). In particular, the three anomeric proton signals (doublets) present in the spectrum of lipid X had chemical shifts and coupling constants almost identical to those in the spectrum of

FIGURE 4:  $^1H$  NMR spectra of (a) lipid X and (b) S-TGD-1.Table 2:  $^1H$  and  $^{13}C$  Chemical Shifts for the Anomeric Carbon of Glycosyl Residues of Lipid X and S-TGD-1

	chemical shift	glucose	mannose	galactose
lipid X	$^1H$	4.95 (3.7 <sup>a</sup> )	4.90 (1.7)	4.46 (7.8)
	$^{13}C$	96.7	98.75	103.74
S-TGD-1	$^1H$	4.97 (3.5)	4.91 (1.8)	4.49 (7.8)
	$^{13}C$	96.8	98.98	103.5

<sup>a</sup> Values in parentheses are coupling constants ( $J$ , Hz).

S-TGD-1 (Table 2). These doublets, centered at about 4.95 ppm ( $J = 3.7$  Hz), 4.90 ppm ( $J = 1.7$  Hz), and 4.46 ppm ( $J = 7.8$  Hz) in both spectra could be assigned to the anomeric protons of  $\alpha$ -glucopyranosyl,  $\alpha$ -mannopyranosyl, and  $\beta$ -galactopyranosyl residues, respectively (5, 16). These results indicate that the polar headgroup of the novel glycolipid is composed of the same sugars in the same sequence and anomeric configuration as in S-TGD-1, namely ( $\beta$ Galp  $\rightarrow$

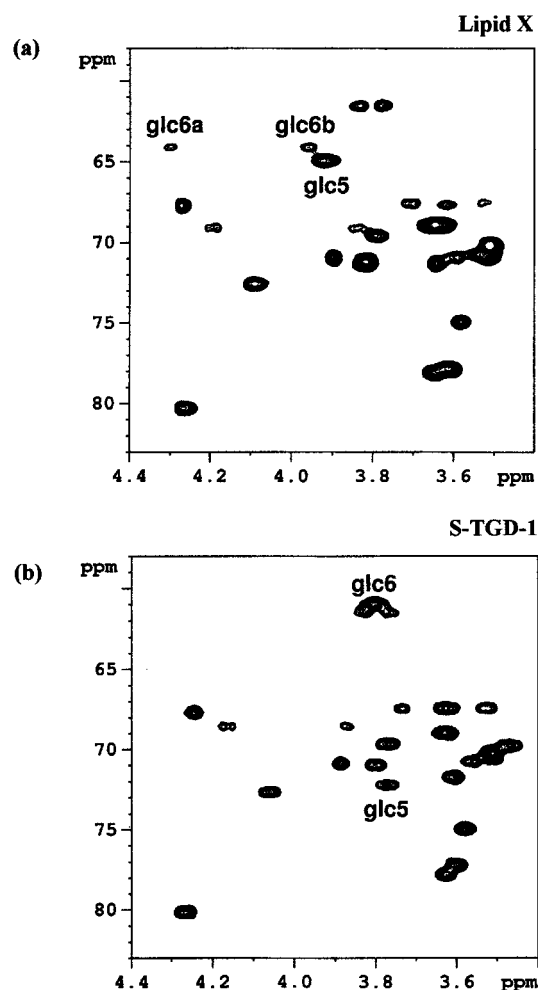


FIGURE 5:  $^1\text{H}$ - $^{13}\text{C}$  heterocorrelated 2D-NMR spectra of (a) lipid X and (b) S-TGD-1 in the sugar region upfield with respect to the anomeric signals.

$\alpha\text{Man} \rightarrow \alpha\text{Glc}$ ), and also that the sulfate group is probably located on C-3 of the galactose residue, as in S-TGD-1 (17).

$^{31}\text{P}$  NMR analysis showed a single phosphorus signal at 2.4 ppm, indicating the presence of one phosphate group in the novel glycolipid molecule, in agreement with the phosphorus analysis data. For comparison, the phosphorus signals for PGP-Me were at 2.1 and 0.9 ppm. The position of attachment of the phosphate group in lipid X could be ascertained by comparison of the  $^1\text{H}$ - $^{13}\text{C}$  heterocorrelated 2D NMR spectra of the novel glycolipid with that of S-TGD-1, supported by DEPT 135  $^{13}\text{C}$  spectral analysis (Figure 5), which showed that both  $^1\text{H}$  and  $^{13}\text{C}$  resonances are very similar in the two compounds. The main differences were (i) the most shielded carbon signal in the sugar region of S-TGD-1 assignable to C-6 of the glucose residue (61.5 ppm) is replaced in the spectrum of the novel glycolipid by a downfield-shifted  $^{13}\text{C}$  signal (64.0 ppm) split into two cross-peaks, due to the diastereotopic splitting of the proton signal (glc6a, 4.30 ppm; glc6b, 3.98 ppm) and (ii) the cross-peak at 72.4 ppm ( $^{13}\text{C}$ ) and 3.78 ppm ( $^1\text{H}$ ) in the spectrum of S-TGD-1 assigned to glucose C-5 is replaced by a cross-peak at 65.2 ppm ( $^{13}\text{C}$ ) and 3.92 ppm ( $^1\text{H}$ ) in the spectrum of the novel glycolipid. These differences suggest that the attachment of the PA phosphate group to S-TGD-1 is at the C-6 position of the glucose residue (see Figure 6a), in agreement with numerous literature data (18–22). Such a

structure would have a molecular mass of 1933.4 calculated for  $\text{C}_{104}\text{H}_{205}\text{O}_{26}\text{PS}$ , in good agreement with the  $m/z$  of the  $[\text{M} - \text{H}]^-$  molecular ion of lipid X (Figure 2a).

Further evidence for a S-TGD/PA-linked structure and the mode and position of attachment of these groups was obtained by examination of the products of acid methanolysis of lipid X (see the Experimental Procedures), compared to those of S-TGD-1 and PGP-Me. Strong acid methanolysis released diphitynylglycerol (DPG; MW 653) as the major hydrophobic product from all three samples; DPG was identified by TLC in solvent C ( $R_f$  0.63; DPG standard, 0.63) and by ESI-MS (positive mode) ( $m/z$  676 =  $[\text{M} + \text{H} + \text{Na}]^+$ , data not shown). In addition, the hydrophobic methanolysis products of lipid X when analyzed by ESI-MS (negative mode) showed two other main ion peaks at  $m/z$  908.0 and 1529.3 (data not shown, but see Figure 7a). The latter ion corresponded to one of the fragmentation ions ( $[\text{M} - \text{HSO}_3 - \text{diglycosyl}]^-$ ) present in the ESI-MS spectrum of lipid X (Figure 2a). The 908.0 ion peak corresponded to the loss of the glycosidically bound diphitynylglycerol residue from the 1529.3 fragment plus methylation of the anomeric OH group ( $[\text{M} - \text{HSO}_3 - \text{diglycosyl} - \text{DPG} + \text{OCH}_3]^- = 1934 - 405 - 651 + 31 = 908$ ). The two lipid hydrolysis products with  $m/z$  1529.3 and 908.0 had  $R_f$  values of 0.96 and 0.73, respectively, on TLC in solvent A (Figure 7a), and both gave a positive test with the sugar and phosphate stains. These data are consistent with the release of  $\text{HSO}_3^-$ -Gal-Man, forming the  $m/z$  1529.3 fragment, followed by release of DPG glycosidically bound to the glucosyl residue of the 1529.3 fragment with concomitant methylation of the glucosyl anomeric OH group, forming the  $m/z$  908.0 fragment molecule (Figure 6a).

Analysis of the water-soluble components of strong acid methanolysis of lipid X and S-TGD-1 showed that the unknown glycolipid released galactose, mannose, and glucose in the mole ratio 1:1:0.5, while, as expected, the known sulfoglycolipid S-TGD-1 released galactose, mannose, and glucose in equimolar proportion. In lipid X, the lower amount of glucose compared to that of the other two hexoses could be explained by the presence of a phosphate group attached to glucose, most likely at the C-6 position, by analogy with lipoteichoic acids in Gram-positive bacteria (23), although attachment of the phosphate group at the C-3 or C-4 position is also possible. However, the greater acid stability of the primary 6-phosphate compared to the secondary 3- or 4-phosphate would favor the linkage at C-6 of glucose. This possibility was confirmed by HPLC analysis of the water-soluble components which identified the phosphorylated hexose as the glucose-6-phosphate (not shown). These data are consistent with the NMR data given above and confirm that lipid X contains the same sugars as in S-TGD-1 but that the glucose residue is phosphorylated at the C-6-position, in support of the structure given in Figure 6a.

Further evidence supporting this structure was obtained from a time course study of the products of mild acid methanolysis of lipid X (see the Experimental Procedures). The products were separated by TLC in solvent A (Figure 7b), and the individual lipid methanolysis products present at 20 h were eluted from the plate and analyzed by ESI-MS (negative mode). With increasing incubation time, an increasing amount of desulfated lipid X ( $m/z$  1853.8) was formed together with lesser amounts of two lipids showing

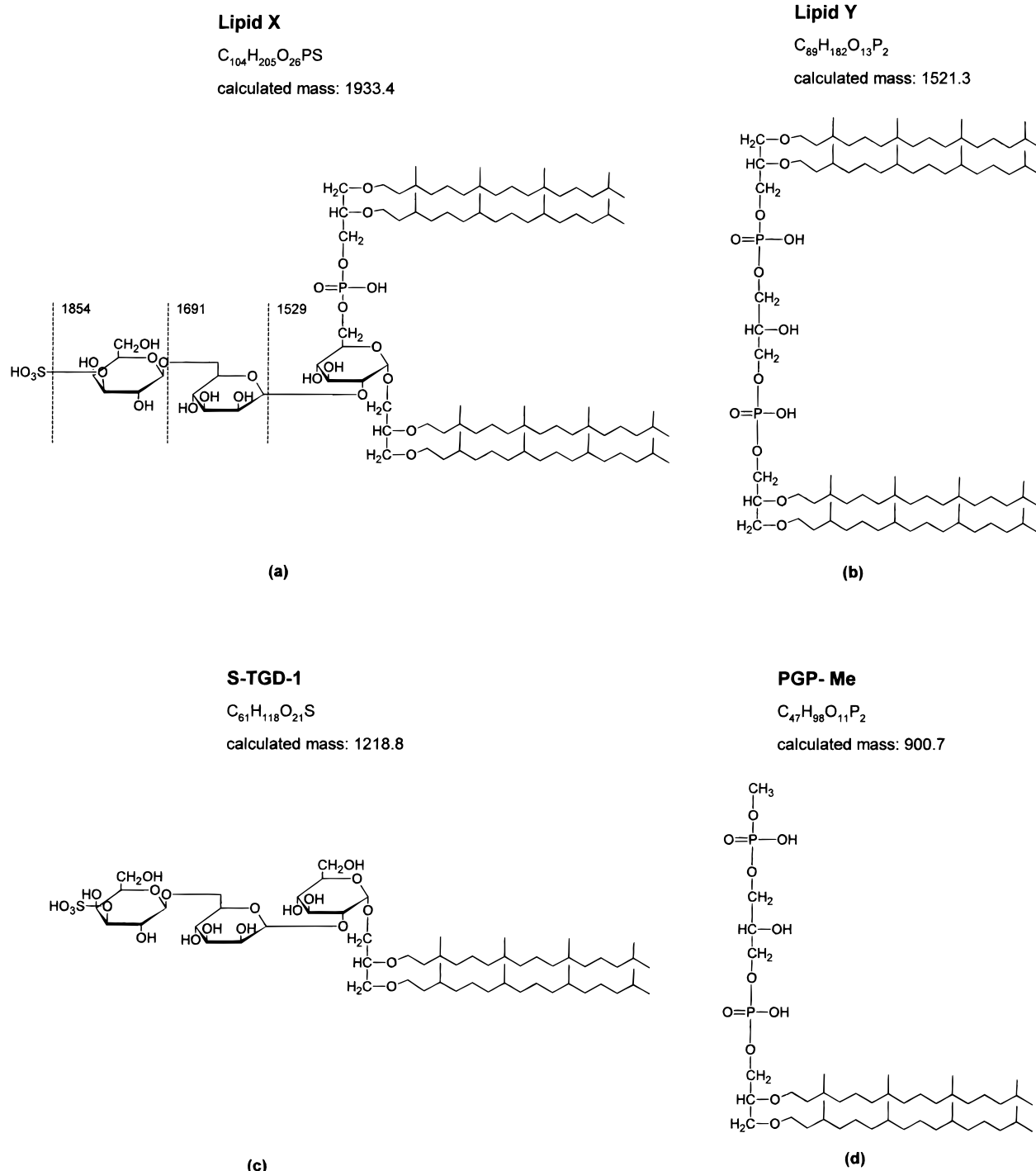


FIGURE 6: Structures of (a) lipid X, (b) lipid Y, (c) S-TGD-1, and (d) PGP-Me. In (a) some of the degradation products of lipid X ( $m/z$  negative ions) are indicated.

ion peaks at  $m/z$  1691.4 and 1529.3. These two lipids stained positively with both the phosphate and sugar stains, and clearly one of them ( $m/z$  1691.4) corresponds to the loss of a sulfomonoglycosyl group and the other ( $m/z$  1529.3) corresponds to the loss of a sulfodiglycosyl group and is the same as that formed on strong acid methanolysis of lipid X (see above). It should be noted that both peaks were also observed as fragmentation ions in the ESI-MS (CID) spectrum of lipid X (Figure 3a). Thus, acid methanolysis of lipid X most likely proceeds as follows: lipid X  $\rightarrow$  lipid X - sulfate ( $m/z$  1854)  $\rightarrow$  lipid X -  $HSO_3$ -Gal ( $m/z$  1691)  $\rightarrow$  lipid X -  $HSO_3$ -Gal-Man ( $m/z$  1529)  $\rightarrow$  lipid X -  $HSO_3$ -

Gal-Man - DPG +  $OCH_3$  ( $m/z$  908) (some of the degradation products are indicated in Figure 6a).

(ii) *Lipid Y*. Lipid Y gave a positive test with the phosphate stain but not with sugar, sulfate, amide, or amino group stains, indicating that it is a phospholipid. TLC in solvent A of purified lipid Y showed a single lipid component (see Figure 2c). On a preparative scale 0.84  $\mu$ mol of lipid Y (in comparison to 6  $\mu$ mol of lipid X) was obtained; the molar ratio lipid Y:retinal of PM lipid extract is therefore 0.12. Its high  $R_f$  (0.94) on TLC in solvent A, compared to that of PG (0.79) (Figure 1), is indicative of the presence of a larger hydrophobic region in lipid Y than in PG. P analysis gave a

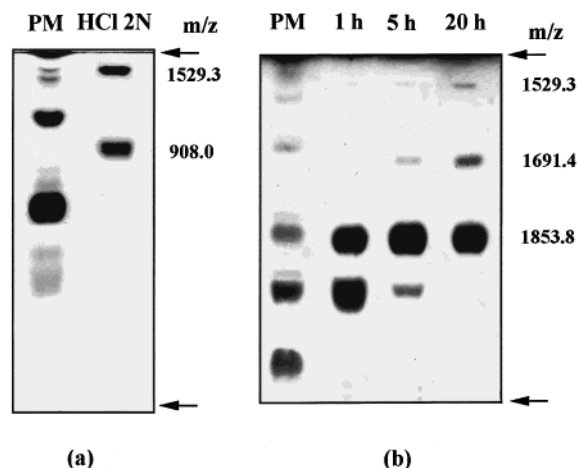


FIGURE 7: TLC plates of the methanolysis products of lipid X (see the procedure given in the Experimental Procedures): (a) strong acid methanolysis (5 h) and (b) mild acid methanolysis time course. TLC plates were developed in solvent A. Numbers reported indicate  $m/z$  values (negative ions) of each isolated spot. Only the lipids positive to phosphate stain are visualized in (a).

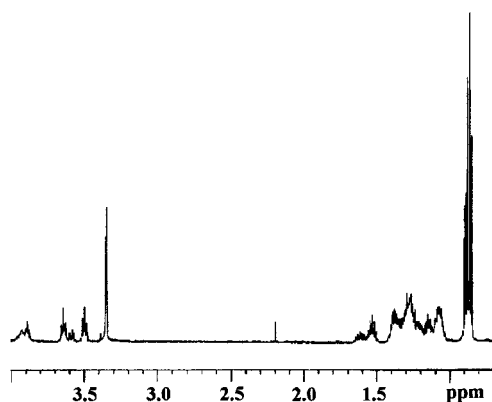


FIGURE 8:  $^1\text{H}$  NMR spectrum of lipid Y.

P:lipid molar ratio of 2 for lipid Y, while the  $^{31}\text{P}$  NMR spectrum showed a single phosphorus signal at 2.0 ppm. This suggests that the two phosphate groups in lipid Y are chemically identical and therefore that this lipid has a highly symmetrical molecular structure.

The proton NMR spectrum of lipid Y (Figure 8) shows a group of resonances in the region 4.0–3.5 ppm which can be assigned to glycerol C-1, C-2, and C-3 protons and phytanyl chain C-1 protons; the phytanyl chain  $\text{CH}_3$ ,  $\text{CH}_2$ , and  $\text{CH}$  proton resonances are in the region 1.7–0.8 ppm. The integral ratio of the glycerol + phytanyl group C-1 proton resonances to the remaining phytanyl group proton resonances gave a value of 0.154 (1:6.5) in good agreement with the ratio of 0.147 (23:156) calculated for a diphytanylglycerol ether analogue of bisphosphatidylglycerol (BPG) (cardiolipin) (see Figure 6b). It should be noted that the corresponding integral ratios calculated for PG and PGP-Me are, respectively, 0.19 (15:78) and 0.22 (17:78).

In the  $^1\text{H}$ – $^{13}\text{C}$  heterocorrelated 2D-NMR spectrum of lipid Y (Figure 9), the downfield group of resonances for the *sn* 2 and *sn* 3 phytanyl chain C-1 protons (C1ph2 and C1ph3, respectively) appear as two triplets at 3.64 and 3.50 ppm, respectively, which the  $^1\text{H}$  COSY spectrum shows to be strongly coupled with the upfield phytanyl chain protons. The remaining downfield resonances can be assigned to the

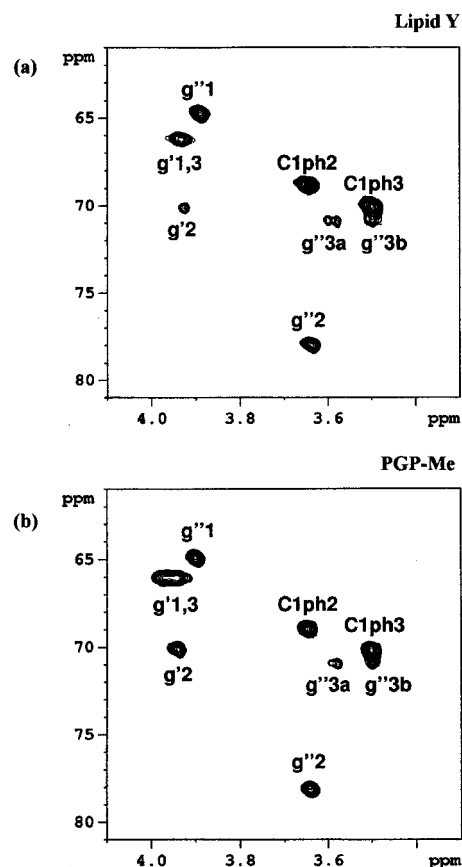


FIGURE 9:  $^1\text{H}$ – $^{13}\text{C}$  heterocorrelated 2D-NMR spectrum of (a) lipid Y and (b) PGP-Me.  $g'$  = central glycerol;  $g''$  = diphytanyl diether glycerols; c1ph2 and c1ph3 = phytanyl C-1 protons.

two kinds of glycerol present in the molecule. The specific assignments of the central diphosphate glycerol ( $g'$ ) and of the two equivalent glycerols of the diether moieties ( $g''$ ) required a combination of  $^1\text{H}$  and  $^{13}\text{C}$  mono- and bidimensional spectral analysis (Figure 9), which shows the assignments for proton and carbon signals derived from the glycerol backbone and phytanyl chain C-1 methylene groups. In particular the assignments of the carbon and proton glycerol backbone signals is supported by  $^{13}\text{C}$  DEPT 135 and  $^1\text{H}$  COSY spectra, respectively (data not shown). The typical downfield shift for the proton and upfield shift for the carbon of the phosphorylated C-1 methylene groups ( $g''1$ ) relative to the unphosphorylated C-3 methylene group ( $g''3a,b$ ) of the two equivalent diether glycerols previously reported (18) should be noted (Figure 9). Moreover, the C-3 hydrogens of glycerol diether show a pronounced diastereotopic splitting with respect to that of the C-1 hydrogens. The glycerol diphosphate moiety shows two resonances which are the most deshielded and nearly synchronous with the proton chemical shift but clearly resolved into two carbon resonances; the most intense of these signals has been assigned to the phosphorylated methylene groups ( $g'1,3$ ) and the other to the C-2 proton ( $g'2$ ). Finally, it should be noted that the  $^1\text{H}$ – $^{13}\text{C}$  heterocorrelated 2D-NMR spectrum of the novel lipid Y is almost superimposable on that of PGP-Me (Figure 9), the only difference being in the relative intensities of the cross-peaks related to the two different kinds of glycerols ( $g'$ ,  $g''$ ) and in the slightly wider proton chemical shift range associated with  $g'1,3$  multiplets due to the asymmetry of the central glycerol C-2 ( $g'2$ ).



ESI-MS of the purified lipid Y (Figure 2b) showed a monocharged molecular ion ( $[M - H]^-$ ) at  $m/z$  1521.3 and a bischarged molecular ion ( $[M - 2H]^{2-}$ ) at  $m/z$  760.0, in good agreement with the molecular mass, 1521.3, calculated for BPG ( $C_{89}H_{182}O_{13}P_2$ ). The major ion peak is that of the bischarged molecular ion at  $m/z$  760.0, the monocharged molecular ion at  $m/z$  1521.3 being a minor peak. The fragmentation ions at  $m/z$  79.1/97.2, 731.7, and 805.9 correspond, respectively, to a  $[PO_3]^-/[H_2PO_4]^-$  ion pair, to PA and to PG, which are compatible with fragments expected to arise from a BPG structure (Figure 6b); all these ion peaks are also present in the BR I and BR II ESI-MS spectra reported in Figure 3.

## DISCUSSION

The present study reveals that, apart from the previously described PM lipids (PGP-Me, S-TGD-I, etc.), two novel archaeal lipids are present in the purple membrane and that these novel lipids are associated with the delipidated bacteriorhodopsin fractions I and II, which are typically isolated after treatment of PM with Triton X-100 followed by phenyl-Sepharose chromatography. These two lipids, a phosphosulfoglycolipid and a diphytanylglycerol analogue of bisphosphatidylglycerol, are most likely involved in the stabilization of isolated delipidated bacteriorhodopsin. Although a complete description of PM lipid composition is beyond the aim of the present study, here we report that the molar ratios phosphosulfoglycolipid:retinal and bisphosphatidylglycerol:retinal are 1 and 0.12, respectively. The molar ratio phosphosulfoglycolipid:retinal is compatible with a role as a stabilizing agent of the trimer structure, while it is difficult at the moment to suggest a similar role for bisphosphatidylglycerol, which appears to be a minor lipid component of PM.

Both novel lipids have two diphytanylglycerol moieties in their molecule, making their structures similar to that of eukaryal cardiolipin (see Figure 6).

It is well-known that the addition of exogenous cardiolipin is essential in preserving the functionality of various mitochondrial membrane transport systems as well as energy transduction systems during solubilization procedures, suggesting that tightly bound cardiolipin is an essential component of the transport activity of carrier proteins (24) and of  $F_0F_1$  ATPase (25). Recently, tightly bound cardiolipin was shown to have a role in stabilizing the quaternary structure of cytochrome *bc* (26). It has also been proposed that cardiolipin may act as a proton buffer and reservoir for participation in proton conduction in energy transducing membranes such as the inner mitochondrial membrane (27). Since both lipid X and lipid Y are bis-negatively-charged amphipathic lipids, like cardiolipin, a similar role may be envisaged for the participation of these two novel lipids in proton pumping of PM.

Several novel cardiolipin analogues have previously been described in bacteria, including glycosylated cardiolipin (28, 29) and lysyl cardiolipins (30), but their cellular function is not known.

The phosphosulfoglycolipid (lipid X) and the diphytanylglycerol analogue of cardiolipin (lipid Y) have not previously been reported present in halobacteria or in PM preparations, although an indication of the presence of traces

of lipid X in PM from *H. halobium* strain S9 can be seen in the ESI-MS spectrum of these PM lipids (14, 15). This previous lack of detection of lipid X may be due to its acid lability (see Figure 7b), particularly to extraction with 5% phosphoric acid, which has been used by some investigators (14), and shown here to be destructive to lipid X (data not shown). The significant solubility of lipid X in acetone used in purification of phospholipids and glycolipids might also explain the previous lack of detection of this lipid. The lack of previous detection of lipid Y could be attributed to its low concentration and its high  $R_f$  on TLC plates, making it difficult to distinguish it from neutral lipids (see Figure 1).

Interestingly the two novel polar PM lipids have also been found in PM isolated from a not yet identified uncultivated halophile strain isolated from the sea saltern facility of Margherita di Savoia in South Italy (unpublished data).

Using our present techniques, it is quite possible that the novel lipids might be found in PMs from other nonengineered strains, since they may not have been detectable with the techniques previously used to study the PM lipids of conventional strains of *Halobacterium*. To determine whether these novel lipids are generally present in PM strains different from those cited above, a detailed examination of lipid patterns from various validated strains obtained from qualified collections is required.

In light of the known biodiversity of members of *Halobacteriaceae* (31), the possibility that other cardiolipin-like analogues may be present in PM from different halobacteria cannot be excluded.

Further studies on the binding properties of lipid X and lipid Y to BR I and BR II and their influence on the light-dependent and proton-pumping activities of BR I and BR II are in progress in our laboratory.

## ACKNOWLEDGMENT

We thank Salvatore E. Carulli of the Department of General and Environmental Physiology for the culture of the microorganism and PM isolation and Vito Linsalata and Enzo Lattanzio of the Institute of Industrial Horticulture—CNR, Bari, for the hexose HPLC analyses.

## REFERENCES

1. Ni, B.F., Chang, M., Duschl, A., Lanyi, J. K., Needleman, R. (1990) *Gene* 90, 169–72.
2. Lopez, F., Lobasso, S., Colella, M., Agostiano, A., and Corcelli, A. (1999) *Photochem. Photobiol.* 69, 599–604.
3. Kushwaha, S. C., Kates, M., and Martin, W. G. (1975) *Can. J. Biochem.* 53, 284–92.
4. Kushwaha, S. C., Kates, M., and Stoeckenius, W. (1976) *Biochim. Biophys. Acta* 426, 703–10.
5. Kates, M. (1990) Glyco-, phosphoglyco-, and sulfoglycolipids of bacteria, in *Glycolipids, Phosphoglycolipids and Sulfoglycolipids* (Kates, M., Ed.) pp 1–122, Vol. 6, Handbook of Lipid Research, Plenum Press, New York.
6. Kates, M., and Kushwaha, S. C. (1995) in *Archaea: A Laboratory Manual, Halophiles* (DasSarma, S., Fleischman, E. M., Eds.) pp 35–54, Cold Spring Harbor Laboratory Press, Cold Spring Harbor, N.Y.
7. Oesterhelt, D., and Stoeckenius, W. (1971) *Nat. New Biol.* 233, 149–52.
8. Bligh, E. G., and Dyer, W. J. (1959) *Can. J. Biochem. Physiol.* 37, 911–917.



9. Kates, M. (1986) *Techniques of Lipidology. Laboratory Techniques in Biochemistry and Molecular Biology*, 2nd revised ed. pp 100–110, 114–115, 153–154, 163–164, 251–253, Vol. 3, Part 2, Elsevier, Amsterdam, The Netherlands, New York.
10. Iida, N., Toida, T., Kushi, Y., Handa, S., Fredman, P., Svennerholm, L., and Ishizuka I. (1989) *J. Biol. Chem.* 264, 5974–80.
11. Bartlett, G. R. (1959) *J. Biol. Chem.* 234, 466–468.
12. Papadopoulos, G. K., Hsiao, T. L., Cassim, J. Y. (1978) *Biochem. Biophys. Res. Commun.* 81, 127–32.
13. Kloppel, K. D., and Fredrickson, H. L. (1991) *J. Chromatogr.* 562, 369–76.
14. Weik, M., Patzelt, H., Zaccai, G., and Oesterhelt, D. (1998) *Mol. Cells* 1, 411–419.
15. Essen, L., Siegert, R., Lehmann, W. D., and Oesterhelt, D. (1998) *Proc. Natl. Acad. Sci. U.S.A.* 95, 11673–8.
16. Dabrowski, J., and Hanfland, P. (1982) *FEBS Lett.* 142, 138–42.
17. Kates, M., and Deroo, P. W. (1973) *J. Lipid Res.* 14, 438–45.
18. Kochanowski, B., Fischer, W., Iida-Tanaka, N., and Ishizuka, I. (1993) *Eur. J. Biochem.* 214, 747–55.
19. Li, Y., and Gary, R. G. (1996) *Biochemistry* 35, 16299–16304.
20. Ferrante, G., Ekiel, I., and Sprott, D. (1986) *J. Biol. Chem.* 261, 17062–17066.
21. Trincone, A., Trivellone, E., Nicolaus, B., Lama, L., Pagnotta, E., Grant, W.D., and Gambacorta, A. (1993) *Biochim. Biophys. Acta* 1210, 35–40.
22. Matsubara, T., Iida-Tanaka, N., Kamekura, M., Moldoveanu, N., Ishizuka, I., Onishi, H., Hayashi, A., and Kates, M. (1994) *Biochim. Biophys. Acta* 1214, 97–108.
23. Fischer, W., Laine, R. A., and Nakano, M. (1978) *Biochim. Biophys. Acta* 528, 298–308.
24. Palmieri, F., Indiveri, C., Bisaccia, F., and Iacobazzi, V. (1995) *Methods Enzymol.* 260, 349–69.
25. Eble, K. S., Coleman, W. B., Hantgan, R. R., Cunningham, C. C. (1990) *J. Biol. Chem.* 265, 19434–40.
26. Gomez, B., Jr., and Robinson, N. C. (1999) *Biochemistry* 38, 9031–8.
27. Kates, M, Syz, J.-Y., Gosser, D., and Haines, T. H. (1993) *Lipids* 28, 877–88.
28. Fischer, W. (1977) *Biochim. Biophys. Acta* 487, 74–88.
29. Peter-Katanilic, J., and Fischer, W. (1998) *J. Lipid Res.* 39, 2286–92.
30. Fischer, W., and Leopold, K. (1999) *Int. J. Syst. Bacteriol.* 49, 653–62.
31. Kamekura, M., and Kates, M. (1999) *Biosci. Biotechnol. Biochem.* 63, 969–972.

BI992462Z